Edinburgh Research Explorer

Multi-objective dynamic optimization of ampicillin batch crystallization: Sensitivity analysis of attainable performance vs. product quality constraint

MULTI-OBJECTIVE DYNAMIC OPTIMIZATION OF AMPICILLIN BATCH CRYSTALLIZATION: SENSITIVITY ANALYSIS OF ATTAINABLE PERFORMANCE VS. PRODUCT QUALITY CONSTRAINTS

Antonios Dafnomilis[a], Samir Diab[b], Alistair D. Rodman[b],
Andreas G. Boudouvis[a], Dimitrios I. Gerogiorgis[b*]

[a] School of Chemical Engineering, National Technical University of Athens, Athens 15780, Greece

[b] Institute for Materials and Processes (IMP), School of Engineering, University of Edinburgh, The Kings Buildings, Edinburgh, EH9 3FB, Scotland, UK

Corresponding Author: D.Gerogiorgis@ed.ac.uk

ABSTRACT

Ampicillin is a broad spectrum antibiotic and World Health Organization *Essential Medicine* whose crystallization is an essential unit operation in its production. A published model for the solubility of ampicillin as a function of pH as well as growth and nucleation kinetics allows for dynamic simulation and optimization of its batch crystallization. While experimental approaches to investigating different dynamic pH profiles have been considered in the literature, dynamic mathematical optimization of pH modulations to meet specific production objectives for ampicillin batch crystallization has yet to be implemented; therein lies the novelty of this study. This work performs dynamic simulation and optimization of the batch crystallization of ampicillin to establish optimal pH trajectories for different production objectives. Simulation of already published batch seeded ampicillin crystallization experiments is performed prior to definition and solution of a dynamic optimization problem for maximization of mean crystal sizes and minimization of size distribution width. The effects of seed loading, time domain discretization and mean crystal size and size distribution width objective function weights are considered and discussed. Pareto fronts showing tradeoffs between different objectives and constraints are then investigated.

1.   Introduction

The discovery and use of antibiotics has resulted in immeasurable benefits to society, revolutionizing modern medicine by treating a vast range of bacterial infections.[1] Global consumption of antibiotics is high, with European and Asian countries consuming the largest volumes of World Health Organization (WHO) countries, shown in Fig. 1. The family of β-lactam antibiotics present one of the most consumed pharmaceutical products globally and are also some of the most important medicines worldwide in terms of their broad applicability to a variety of ailments.[2] Penicillins, a subclass of the β-lactam antibiotic family, are considered critically important to the world healthcare system. Efficient manufacturing of these societally-essential pharmaceutical products is crucial to meet increasing antibiotic demands and for sustainable production.[3]
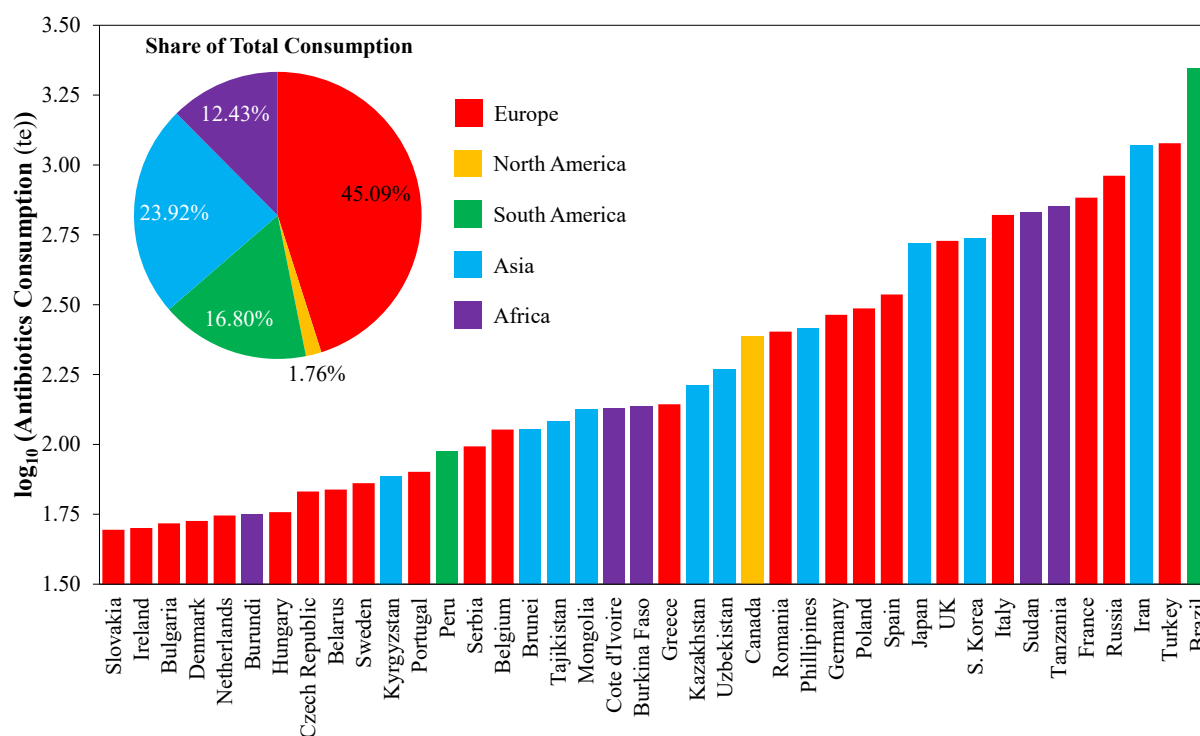

Figure 1: Top 40 World Health Organization (WHO) countries by antibiotic consumption in 2016.[4]

Ampicillin is a broad-spectrum, semi-synthetic β-lactam antibiotic, used to treat various bacterial infections such as urinary and respiratory tract infections, being one of the ten most consumed antibiotics worldwide. Ampicillin is stable against hydrolysis by a variety of β-lactamase enzymes and can therefore be administered for a wide range of gram-positive and -negative infections. Like most high sales volume β-lactam antibiotics, it is manufactured via batch enzymatic synthesis.[5] Design of efficient separation processes of ampicillin is important for lean and effective manufacturing.

Crystallization is an essential process in the pharmaceutical industry for the separation of intermediates or as the final process in the production of an Active Pharmaceutical Ingredient (API).[6] Supersaturation, i.e., the condition where the equilibrium solubility value of the solute is below that of its concentration in the solution, is the thermodynamic driving force for crystal nucleation and growth. Supersaturation can be generated in a variety of ways;

1. reducing temperature, i.e., cooling crystallization
2. removing solvent, i.e., evaporative crystallization
3. altering the solution composition via acid, base or antisolvent addition.

The final size, shape and form of the product crystals influences not only downstream operations but also the physical and chemical properties of the solid product.[7] These properties often represent important quality attributes in the pharmaceutical manufacturing process, e.g., polymorphism and size distribution may affect the bioavailability of the crystalline product.

Table 1: Literature demonstrations of mathematical optimization of pharmaceutical crystallization utilizing population balance modelling to meet specific production objectives.

#	API	Application	Operating Mode	Continuous Design	Objective Function	Method of Supersaturation Generation	No. Stages	Operation / Residence Time (min)	Yield (%)	Benefits Attained	Literature Reference
1	Lovastatin	Blood cholesterol reduction	Batch	(–)	Size distribution control	Antisolvent + Cooling	1	60	NS	Improved size distribution control	Nagy et al., 2008[8]
2	Aspirin	Analgaesic	Batch	(–)	Minimize batch duration + Size distribution control	Antisolvent + Cooling	1	21.6	NS	Reduced fines formation and size distribution control	Lindenberg et al., 2009[9]
3	Flufenamic Acid	Analgaesic	Continuous	PFC	Maximize crystal size + Minimize size distribution width	Antisolvent	4	1.45	93.0	Larger crystal size + narrower distribution width	Ridder et al., 2014[10]
4	Paracetamol	Analgaesic	Batch	(–)	Size distribution + shape control	Cooling	1	90	NS	Improved control of size distribution and shape	Acevedo et al., 2015[11]
5	L-Asparagine Monohydrate	Amino acid	Continuous	PFC	Size distribution control	Cooling	4	100	76.4	Improved size distribution control	Rasche et al., 2016[12]
6	Cyclosporine	Immunosuppressant	Continuous	MSMPR	Maximize yield / purity	Cooling	5	900	85.0	Improved yield and purity	Li et al., 2017[13]
7	Cyclosporine	Immunosuppressant	Continuous	MSMPR	Minimize total costs	Cooling	1	6,456	68.4	Cost optimal design	Diab and Gerogiorgis, 2018[14]
8	Paracetamol	Analgaesic	Continuous	MSMPR	Minimize total costs	Cooling	1	646.8	73.9	Cost optimal design	Diab and Gerogiorgis, 2018[14]
9	Aliskiren	Anticoagulant	Continuous	MSMPR	Minimize total costs	Cooling	1	368.4	83.2	Cost optimal design	Diab and Gerogiorgis, 2018[14]
10	Paracetamol	Analgaesic	Continuous	COBC	Minimize total costs	Antisolvent + Cooling	1	14.93	70.0	Cost optimal design	Jolliffe and Gerogiorgis, 2018[15]
11	Aspirin	Analgaesic	Batch	(–)	Minimize degradation product concentration	Cooling	1	200	90.0	Maximum crystal growth with minimal product degradation	Pal et al., 2019[16]

NS: Not specified

Significant advances in API crystallization design and control have been made in recent decades. Efforts in the development of batch crystallization processes for control of polymorphism, preferential crystallization of enantiomers from racemic mixtures, crystal size and distribution, slurry transfer and integration with membrane separation units, as well as the development of different continuous crystallization technologies have furthered pharmaceutical crystallization significantly.[7] Performing conceptual crystallization process modelling and optimization prior to expensive and time-consuming experimental campaigns allows rapid design space investigation and elucidation of promising process configurations and design and operating parameters.

Model-based optimization of crystallization processes has been implemented in the literature in a variety of ways, e.g. maximizing the product yield and mean crystal size, or minimizing batch/residence time and width of the Crystal Size Distribution (CSD). Other possibilities include minimizing cost or maximizing total profit.[14,15,17] Table 1 summarizes instances of process optimization for pharmaceutical crystallization processes in order to meet specific production objectives (e.g., maximize crystal size, minimize size distribution width, enhance economic performance etc.), utilizing mathematical modelling and population balance equations from the literature. Most optimizations use cooling profiles and/or antisolvent addition rates for supersaturation control to meet the desired objectives. A variety of batch crystallizer optimization studies have been implemented (Table 1) as well as several recent implementations of optimization towards continuous crystallizer design, including traditional Mixed Suspension, Mixed Product Removal (MSMPR) and Plug Flow Crystallizer (PFC) units, as well as more elaborate Continuous Oscillatory Baffled Crystallizer (COBC) designs.

The crystallization of ampicillin has been demonstrated in the literature by pH-variation, including a model with detailed growth and nucleation kinetics and solubility as a function of pH, allowing detailed prediction of attainable crystallization yields and mean crystal sizes for different pH variation profiles and seeding conditions.[18] Dynamic optimization of pH-profiles for the batch crystallization of ampicillin subject to various product specifications and operational constraints may present improved process performances vs. straightforward linear pH variations demonstrated in the literature thus far.[19]

In this work, the recently published crystallization model for ampicillin is utilized for dynamic optimization of pH manipulation profiles over the batch runtime in order to optimize product quality attributes subject to different operational and performance constraints.[18] The paper is structured as follows. First, the published dynamic model for the batch crystallization of ampicillin that is used in this work for optimization purposes is described in detail. The performance of different demonstrated crystallization cases from the same previously published work are then presented. The formulation of a dynamic optimization problem with pH as the manipulated (control) variable is described, with different case studies corresponding to experimental demonstrations is then described. Optimization results for different considered cases are then presented with a critical comparison of the outcomes versus the published demonstrations. Tradeoffs between different product quality attributes are examined and discussed in the context of the implemented methodology.

2.   Methodology
2.1.   Dynamic Modelling of Batch Crystallization
The batch crystallization of ampicillin is modelled using published solubility = f(pH), growth and nucleation kinetics and population balances.[18] The following assumptions are made in the model:

- The feed stream is a clear mother liquor with dissolved ampicillin for crystallization with seeds
- Crystal breakage and agglomeration do not occur
- Growth is size-independent and linear.

The implemented crystallization model describes growth and nucleation kinetics, API solubility, crystal population balances and mass balances. The simultaneous solution of these equations describes batch crystallization. In this work the crystalliser is considered isothermal at temperature, $T = 298.15$ K. Crystallization is induced only due to the solubility change by pH variation. It is also assumed that pH variation in the mother liquor mixture is instantaneous.

2.1.1. Crystallization Kinetics

Crystal growth and nucleation kinetics are described by the eqs. 1–5. Crystal growth rate terms (eq. 1) consist of G = linear crystal growth rate, k_G = crystal growth pre-exponential factor, SS = supersaturation (eq. 5) and g = crystal growth exponent. Nucleation terms (eqs. 2–4) are J = overall nucleation rate composed of B_1 and B_2 = primary and secondary nucleation rates, respectively, k_B = nucleation pre-exponential factors, B_0 = primary nucleation constant, M = suspension density, b = suspension density exponent and s = secondary nucleation exponent. Supersaturation, SS (eq. 5), is calculated as the ratio of the ampicillin concentration in solution, $[Amp]$, to the solubility value, S. Growth and nucleation rates, as well as supersaturation, vary as a function of time, t, in the batch crystalliser.

$$G(t) = k_G \left(SS(t) - 1 \right)^g \tag{1}$$

$$J(t) = B_1(t) + B_2(t) \tag{2}$$

$$B_1(t) = k_{B1} \exp\left(-\frac{B_0}{\ln(SS(t)^2)} \right) \tag{3}$$

$$B_2(t) = k_{B2} M(t)^b \left(SS(t) - 1 \right)^s \tag{4}$$

$$SS(t) = \frac{[Amp](t)}{S(t)} \tag{5}$$

The suspension density is calculated via a mass balance on ampicillin between mother liquor (aqueous solution) and crystalline product (solid) phases (eq. 6),

$$M(t) = m_{sol}\left([Amp](t_0) - [Amp](t) \right) \tag{6}$$

where $t_0 = 0$ is the batch start time and m_{sol} is the mass of the mother liquor solution. Crystallization kinetic parameters are summarized in Table 2. Nucleation and growth kinetic parameters for ampicillin crystallization have been regressed in the literature from a variety of experiments.[18] Primary nucleation parameters (k_{B1}, B_0 in eq. 3) are regressed from induction time experiments under a variety of supersaturations, wherein supersaturation is rapidly induced by acid addition to a crystal-free solution of ampicillin (aq.) and the induction time is considered that taken to form nuclei (size range 0–10 μm); full details of the experiments are found in the literature.[18] The regressed parameters k_{B1} and B_0 showed good fit to experimental data, with a coefficient of determination $R^2 > 0.98$ (experimental data and model fit visualized in Fig. 5 of Encarnación-Gómez et al.[18]). The remaining crystallization kinetic parameters (growth parameters k_G and g in eq. 1, secondary nucleation parameters k_{B2}, b and s in eq. 4) have been regressed via different seeded and unseeded experiments with varying initial supersaturations, initial pH and final pH for linear pH decrease. The full set of crystallization kinetic parameters replicated concentration profiles and final Mean Crystal Sizes (MCS) well.

Table 2: Crystallization kinetics model parameters.[18]

Symbol	Value	Units
k_G	8.95×10^6	m min^{-1}
g	1.87	—
B_0	1.27	—
k_{B1}	5.0×10^9	# crystals (g kg^{-1})$^{-1}$ min^{-1}
k_{B2}	2.2×10^9	# crystals (g kg^{-1})$^{-1}$ min^{-1}
b	0.60	—
s	1.37	—

2.1.2. Ampicillin Solubility

The extended Pitzer model[20] is used to describe ampicillin solubility as a function of pH,

$$\log \frac{S(pH)}{S(pI)} = pI - pH + \log\left[\frac{1 + 10^{pH - pK_{A1}}}{1 + 10^{pI - pK_{A1}}} \right] + \log\left[\frac{1 + 10^{pH - pK_{A2}}}{1 + 10^{pI - pK_{A2}}} \right] + \frac{2}{\ln 10} \lambda [S(pI) - S(pH)] \tag{7}$$

$$\lambda = \frac{2\pi\sigma^3 N_A \rho}{3}\left(1 - \frac{\varepsilon}{k_B T}\right) \tag{8}$$

where constants ε, σ, pK_{A1} and pK_{A2} are taken from the literature for ampicillin solubility description = f(pH), k_B is the Boltzmann constant, N_A is the Avogadro number, ρ is the density of ampicillin and T is temperature; parameters for eqs. 7–8 are summarized in Table 3. The parameters presented on Table 3 are used in eqs. 7–8 to calculate the solubility of ampicillin as a function of pH. Eq. 7 is an implicit function with respect to the solubility of ampicillin, solved numerically using the nonlinear equation solver fzero in MATLAB. The model accurately describes solubility as a function of pH; Fig. 2 illustrates ampicillin solubility described by the extended Pitzer model as well as experimental data points from the literature.[18,21,22] The solubility of ampicillin at the isoelectric point, $S(pI)$, was regressed such that the model agreed with the published extended Pitzer model results (Table 3).[18]

Table 3: Parameters for the extended Pitzer and solubility models at 298.15 K.

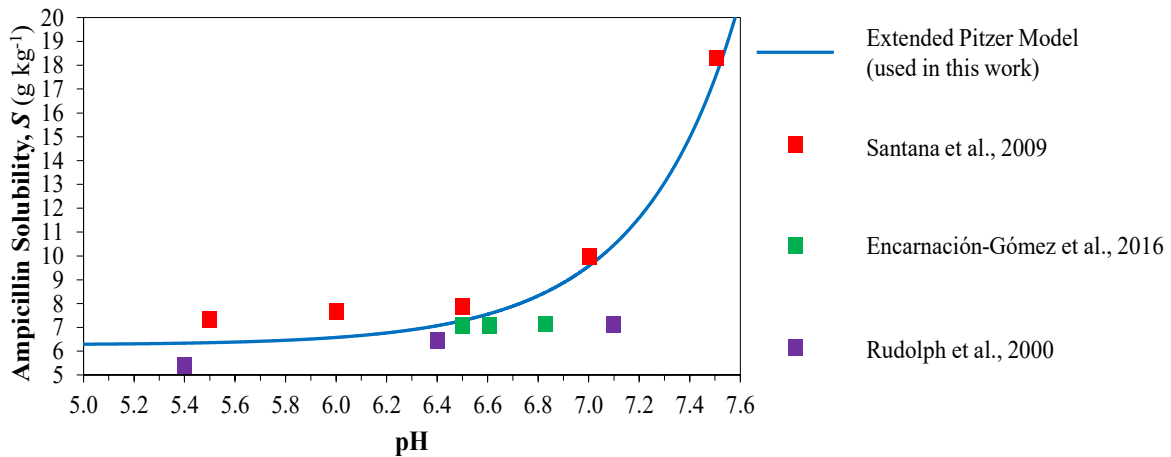| Symbols	Value	Units	Reference
σ	5.42×10^{-10}	m	[18]
ε/k_b	336.18	K	[18]
pK_{A1}	2.14	–	[23]
pK_{A2}	7.31	–	[23]
pI	$(pK_{A1} + pK_{A2}) / 2 = 4.725$	–	This work
$S(pI)$	0.018	mol kg^{-1}	This work

Figure 2: Aqueous ampicillin solubility as a function of pH predicted by the extended Pitzer model.[20]

2.1.3. Population and Mass Balance Equations

The population balance equation for a batch crystalliser with no agglomeration or breakage is described by eq. 9, where n is the population density function, L, is the characteristic 1D crystal length (as growth is assumed linear). The assumption of 1D crystal growth is appropriate, as the ampicillin trihydrate crystal morphology is needle-like from the reported crystallization experiments.[18] The boundary condition (eq. 10) is the nuclei population density, while the initial condition, n_0 (eq. 11) is the initial population balance at time $t = 0$. For seeded crystallization, n_0 is the population density of the seeds.

$$\frac{\partial n(t, L)}{\partial t} = -\frac{\partial\big(G(t)n(t, L)\big)}{\partial L} \tag{9}$$

$$n(t, 0) = \frac{J(t)}{G(t)} \tag{10}$$

$$n(0, L) = n_0 \tag{11}$$

The solute mass balance is calculated as the change in suspension density, assuming that the volume of the crystals is much smaller than that of the mother liquor.

5

$$\frac{d[Amp]}{dt} = -\frac{dM}{dt} \tag{12}$$

The system of PDEs composing the population density functions are converted to a system of ODEs via the method of moments,[24,25] often used to simplify crystallization population balance modelling in crystallization models. The moments of the distribution are calculated by eq. 13, integration of which leads to the system of ODEs containing crystallization kinetic terms (eqs. 14 and 15). The mass balance is then obtained from eq. 16

$$m_i = \int\limits_0^\infty n(t, L) L^i dL \tag{13}$$

$$\frac{dm_0}{dt} = J \tag{14}$$

$$\frac{dm_i}{dt} = iG m_{i-1} \tag{15}$$

$$\frac{d[Amp]}{dt} = -k_v \rho_C \frac{dm_3}{dt} = -3 k_v \rho_C G m_2 \tag{16}$$

where ρ_c is the crystal density (= 1.5 g cm^{-3}) and k_v the crystal volume shape factor (= 0.03).[18] The system of ODEs describing the population balance model is solved using MATLAB's ODE solver ode113.

The Mean Crystal Size (*MCS*) is calculated from the zeroth and first moments (eq. 17).

$$MCS(t) = \frac{m_1(t)}{m_0(t)} \tag{17}$$

Although implementing the method of moments presents a computationally simpler approach to crystallization modelling, the full crystal size distribution information is lost in the transformation. The standard deviation, *STD* (eq. 18), quantifies the width of the size distribution without its explicitly calculation; low values of *STD* correspond to narrow size distributions. Another metric often used to quantify the width of size distributions is the Coefficient of Variation, *CV* (eq. 19)

$$STD = \frac{m_2(t_f)}{m_0(t_f)} - \left(\frac{m_1(t_f)}{m_2(t_f)}\right)^2 \tag{18}$$

$$CV = \sqrt{\frac{m_2(t_f)\, m_0(t_f)}{m_1^2(t_f)} - 1} \tag{19}$$

2.2. Dynamic Simulation

Prior to formulation of a dynamic optimization problem for ampicillin crystallization, we first discuss and illustrate the experimentally demonstrated performances from the literature.[18] Here, we consider three seeded ampicillin crystallization cases as performed in the literature, whose details are summarized in Table 4. Seeding a crystallization process is a simple method to control supersaturation in a batch crystallizer and to attain a specific mean crystal size and distribution width.[26]

Table 4: Summary of experimentally demonstrated cases considered in this work.

Parameter	Case 1	Case 2	Case 3
Seed Loading (wt%)	1.8	3.0	15.0
pH$_0$	7.09	7.01	6.84
pH$_f$	6.33	6.40	6.51
ΔpH (hr^{-1})	1.50	1.40	0.60
t_f (hr)	4.23	5.83	25.00

Previous work by Encarnación-Gómez et al.[18] performed three seeded batch ampicillin crystallization experiments with varying initial and final pH, rate of linear pH decrease, batch duration (t_f) (implemented by the authors) and seeding concentration = {1.8, 3.0, 15.0} wt%.[18] Fig. 3 shows the implemented pH trajectories, ampicillin (mother liquor) concentration profiles and crystallization performances (i.e., crystallization yield and *MCS*). The final batch time, t_f, varies significantly between cases; thus, the time domains have been normalised with respect to final batch times for each case, which are also shown in Fig. 3. The presented results use the crystallization model equations described in sections 2.1–2.3 and have been validated vs. the original model results.[18]
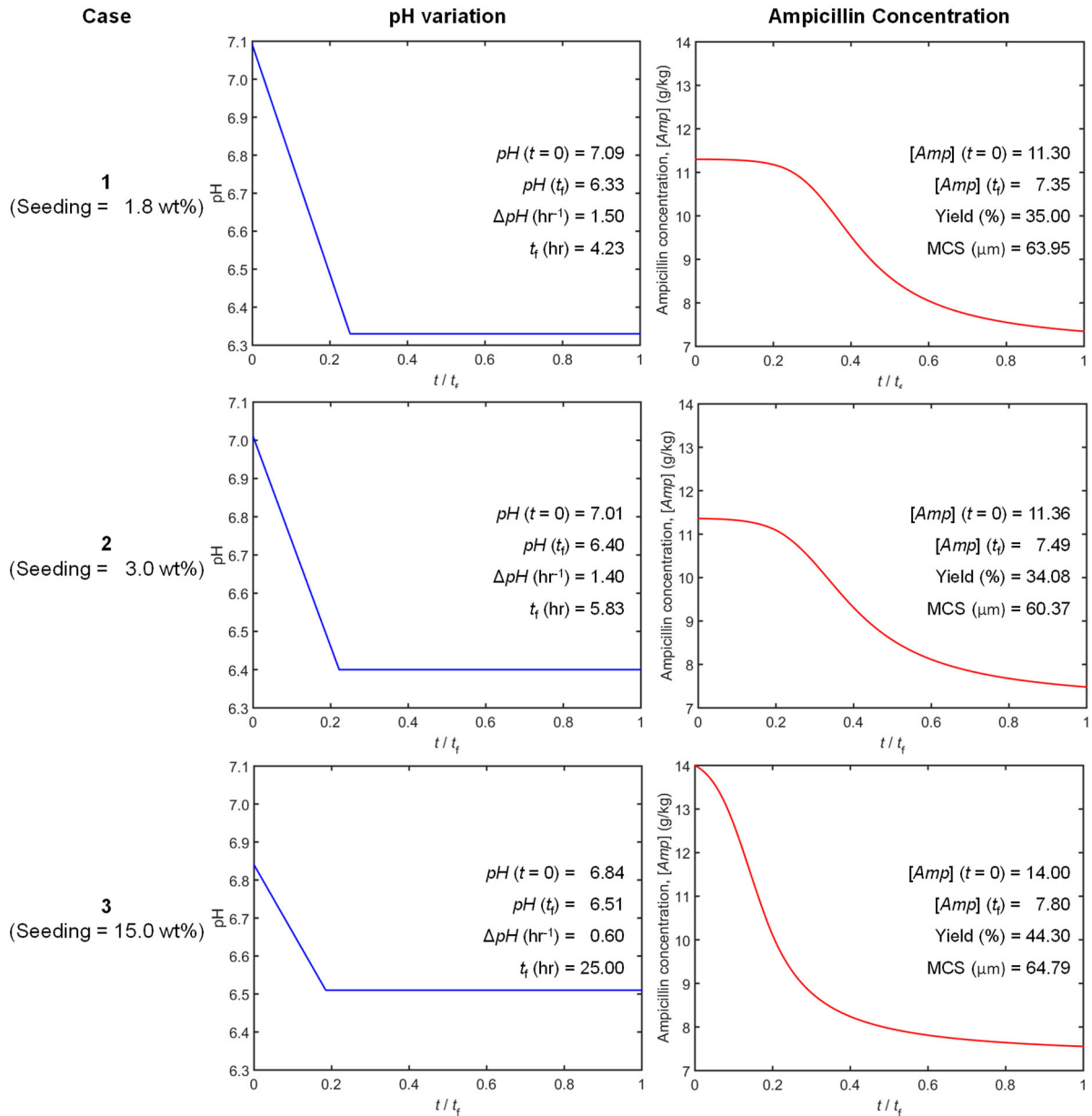

Figure 3: Dynamic simulation results for seeded cases from the literature.

Fig. 3 shows that when seeding concentration and initial concentration are high and when the pH change is slightly lower (Case 3 vs. 1 and 2), crystallization yield increases by nearly 10%, while *MCS* only varies within a range of 5 μm (60–65 μm). The effect of different experimental conditions on the size distributions are not discussed as experimental data was not provided in the original work, nor can they be gained from the model equations (i.e., moments), as described previously. The calculated concentration profiles are exactly those in the literature as per the model equations and agree with the experimental data as per reported experimental results (Fig. 11 in Encarnación-Gómez et al.[18]).

Experimental results for CSD are not reported in the literature, but modelled final MCS values agree with experimental values with relative errors of –0.12% for Case 1 and –16.56% for Case 3 (the final experimental MCS value for Case 2 was not reported in the literature). These errors agree with the modelled result discrepancies reported in the literature.

The pH profiles investigated in the experiments in the literature are linear only and do not consider other dynamic trajectories which could lead to enhanced process benefits, e.g., higher yields, larger *MCS*, lower *CV* etc.[27] Control (pH) trajectory optimization for different objectives has not yet been implemented in the literature for ampicillin crystallization and could yield process benefits over the experimental demonstrations described here. Thus, dynamic pH optimization as per the methodology described in section 2.4, is implemented.

2.3. Dynamic Optimization
2.3.1. Problem Formulation

The purpose of dynamic optimization is to establish a control variable trajectory as a function of time to meet some objective regarding the system state variables. This work considers the dynamic optimization of the batch seeded crystallization of ampicillin by manipulation of the pH trajectory over the batch duration. Generally, large mean crystal sizes and narrow size distributions are desirable crystal product quality attributes prior to further downstream processing. In this work, we aim to maximize *MCS* while simultaneously minimizing the width of the crystal size distribution, quantified by *STD*. This is implemented by considering the objective function as the minimization of a weighted sum of *STD* and *MCS*, with associated weights W_{STD} and W_{MCS}. Values of *STD* and *MCS* are scaled by 10^{10} and 10^6, respectively, in the objective function formulation to ensure they are of the same order of magnitude to ensure ease of convergence and numerical stability. Imposed constraints on the problem are also defined.

$$\min_{pH(t),t_f} f(x, t_f) = W_{STD}STD - W_{MCS}MCS \tag{20}$$

$$7 \leq pH(t_0) \tag{21}$$

$$5.5 \leq pH(t) \leq 8.0 \tag{22}$$

$$[Amp](t_f) \leq [Amp]_{target} \tag{23}$$

$$1 < SS(t) \tag{24}$$

The first constraint (eq. 21) ensures the initial pH value is greater than 7.0 to ensure sufficient supersaturation at the beginning of the batch duration. The second constraint (eq. 22) ensures pH is not too low (leading to ampicillin degradation) or high (leading to undesirable non-trihydrate ampicillin polymorphs). Ampicillin has limited chemical stability at pH ≤ 5, below which degradation products are formed.[28] Batch enzymatic reactor effluents for ampicillin synthesis are typically round pH = 6.0–6.5.[29,30] It is preferred that ampicillin crystallization occurs at pH < 8 to ensure it crystallizes in the desired trihydrate polymorph[31] and to avoid excessive supersaturations inducing uncontrolled nucleation resulting in broad size distributions. The third constraint (eq. 23) ensures that a minimum of a target amount of ampicillin has been crystallised from solution, which varies between the considered experimental cases; considered values and their corresponding crystallization yields are shown in Table 5. Considered crystallization yields are comparable with those attained in experimental demonstrations;[18] moreover, we consider a range of crystallization yields to quantify tradeoffs between yield and *MCS* and *CV*. The fourth constraint (eq. 24) ensures crystallization occurs by maintaining sufficient supersaturation (interior point constraint). The average seed crystal size used in this work is $\bar{L}_{seed}$ = 74.0 μm as per the experimental demonstration in the literature.

Table 5: Different product ampicillin concentration constraints and batch durations for each case.

Case	1	2	3
Seeding (wt%)[18]	1.8	3.0	15.0
$[Amp](t_f)$ (g kg^{-1})	{6.6, 6.8, 7.0, 8.0, 9.0}	{6.6, 6.8, 7.0, 8.0, 9.0}	{11.0, 9.0, 7.5, 6.9, 6.7, 6.5}
Yield (%)	{41.6, 39.8, 38.1, 29.2, 20.4}	{41.9, 40.1, 38.4, 29.6, 20.8}	{53.6, 52.1, 50.7, 46.4, 35.7, 21.4}
t_f (min)	250	350	1,500

2.3.2. Solution Method

In this work, a direct method for dynamic optimization (simultaneous strategy) has been performed. Orthogonal polynomials on finite elements were used to approximate the control (pH) and state (moments and ampicillin concentration) trajectories allowing the continuous problem to be described as a Nonlinear Programme (NLP). The state trajectories (moments and ampicillin concentration) are described by eqs. 13–16, which encompass the solubility trajectory (= function of implemented pH control profile), crystallization kinetics and population and mass balance equations. The dynamic optimization has been performed using the DynOpt package for MATLAB.[32] Control and state variables are discretized via Lagrange polynomials, the coefficients of which become decision variables to a larger NLP problem. Differential equations are converted into algebraic equations using collocation on finite elements. The final NLP problem consists of the converted ODEs, continuity equations for the state variables and any other equality and inequality constraints that may be required. The problem is then solved using an NLP solver; the NLP solver used in this work is MATLAB's fmincon. The dynamic batch crystallization process is described by a highly non-convex and nonlinear system of differential algebraic equations. The dynamic optimization solver is a local solver and does not guarantee global optima for any of the presented cases.

A graphical representation of the model is provided in Fig. 4. The time interval t is discretized into different t_i segments with each being of a length Δt_i, $u(t)$ is the control variable and $x(t)$ is the state variable matrix. The real value of $x(t)$ with regards to the changing control variable is presented as a solid curve. In DynOpt, $x(t)$ is approximated over each element i, $t_i \leq t \leq t_{i+1}$ by a Lagrange polynomial. The approximation $x_{Kx}(t)$ is a (K_x+1) degree polynomial, where K_x is the number of collocation points. The same principle can be applied to $u(t)$ where it is approximated by $u_{Ku}(t)$, a K_u degree polynomial, where K_u is the number of collocation points. In Fig. 4 three collocation points $x_{i,1-3}$ are depicted for the state variable and two points $x_{i,0}$ and $x_{i+1,0}$ at the bounds of the time interval are specified. This amounts to five points in total, between which a fourth order polynomial can be approximated. The locations of the collocation points are the shifted roots of Legendre polynomials. For u_{Ku} only the collocation points are used, as a result these profiles are constrained or bounded only at the collocation points. If $K_u = 1$, the control variable is constant in each time interval, i.e. a Piecewise Constant (PWC) control profile. If $K_u = 2$ the control variable is approximated with a line meaning a Piecewise Linear (PWL) control profile. In order to verify the accuracy of the approximation of the state variables (which depends on the model and degree of discretization), after the optimized profile for the control has been specified, it is advantageous to solve the model using that profile with an ODE solver and verify the accuracy of the DynOpt approximation.
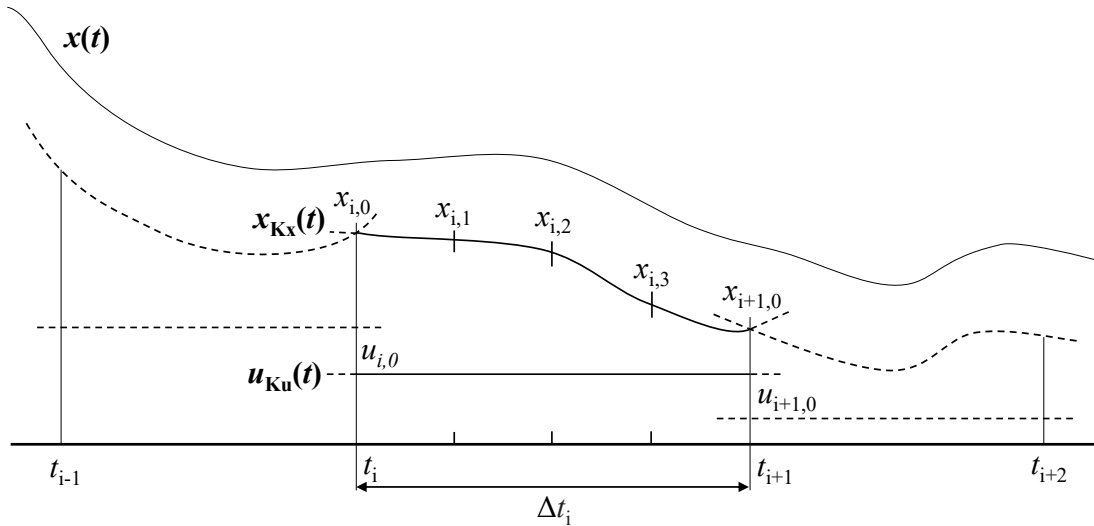

Figure 4: Graphical representation of the method of orthogonal collocation on finite elements.

2.3.3. *Optimization Problem Structure*

In order to improve the accuracy of DynOpt the analytical derivatives of the ODEs, constraints and objective function were provided to the problem model. The time domain is discretized into $N = \{10, 20, 30\}$ intervals. Three collocation points were used to approximate the state variables, while one collocation point was used for the control (pH) variable, i.e., PWC control trajectories. Each case was initialized at a constant pH of 7 across the whole trajectory. Certain instances with constant pH = 7 initialization lead to non-convergence, in which cases an initialization profile of constant pH = 6 is used.

The state variables (i.e., the moments and ampicillin concentration) of the considered system significantly vary in magnitude. Scaling of each moment was implemented as per eq. 25.

$$\overline{m}_i = \frac{m_i}{p_i} \tag{25}$$

where $\overline{m}_i$ is the scaled i^{th} moment, and p_i is the corresponding scaling parameter. The scaling parameters used for each moment are $p_0 = 10^9$, $p_1 = 10^5$, $p_2 = 1$, $p_3 = 10^{-4}$.

In order to ensure that the calculated quality attributes and $[Amp](t_f)$ correspond to realistic values for the state variables, every optimized pH profile was used to simulate the model in MATLAB. Dynamic optimization problems were compared versus simulations using the solution profiles to see if the NLP approximation of the problem was sufficient; in the cases where the approximation was insufficient, the optimization was recomputed using $K_X = 6$ collocation points for the state variables. In some cases of tighter constraints on final ampicillin concentration in solution, the optimization struggled to converge, in which case the system was initialized at a constant $pH = 6$. Such cases of differing initialization are highlighted in the results section.

Objective function weights of $[W_{STD}\ W_{MCS}] = \{[1.0\ 0.5], [1.0\ 1.5]\}$ are also considered. Additionally, the effect of the time discretization, $N = \{10, 20, 30\}$ is considered; varying N changes the number of equispaced time segments in which the pH is piecewise constant. With three experimental cases, each with three discretization levels, each with two combinations of objective function weights for five crystallization yield cases, the total number of optimization problem instances = $3\times3\times2\times5 = 90$.

3.   Results and Discussion
3.1.   Optimal Control Trajectories

PWC profiles between discrete time points were computed in order to investigate the effect of different objective function weight parameters and the degree of discretization. Three options of discretization levels, $N = \{10, 20, 30\}$, have been considered and different combinations for the weights of the objective function have been tested: $W_{STD} = 1.0$ and $W_{MCS} = \{0.5, 1.5\}$. Figs. 5–7 show the optimal pH (control), SS and MCS profiles over the batch duration for different cases (seed loading, N). Figs. 5 – 7 only show results for certain $[Amp]_{\text{target}}$ endpoint constraints and $W_{MCS} = 1.5$; control and state trajectories for the full set of conditions listed in Table 5 are provided in the Supporting Information.

Optimal pH, SS and MCS profiles for different N for Case 1 are shown in Fig. 5. For lower crystallization yields (i.e., higher target ampicillin solution concentrations), the general form of the pH profile is a drop in pH near the beginning, followed by an increase and then a drop towards the end of the batch duration. This form of pH (control) profile results in a high supersaturation at the start of the batch, followed by a decrease and then another increase towards the end. The initial high SS value at the start of the batch promotes nucleation over growth. The subsequent low supersaturation allows nucleated crystals to grow in order to attain high MCS as per the defined optimization objective function. The final increase in supersaturation allows for further nucleation of crystals in order to increase the yield to meet the imposed concentration constraint. This results in MCS profiles which drop at the start (as many nuclei form, the MCS decreases) followed by an increase (due to growth dominating). As the target crystallization yield is increased, the resulting optimal control and state profiles change. The initial pH drop and increase in order to stimulate nuclei followed by growth, respectively, remain consistent trends with lower target crystallization yields; however, the final decrease in pH in order to enhance the yield occurs earlier. This behavior is caused by the need to crystallise more nuclei in order to meet the target yield. As a consequence, the MCS profiles begin to gradually decrease due to the formation of nuclei, although they are maintained at fairly high values and approximately the same as for cases with lower target crystallization yields.
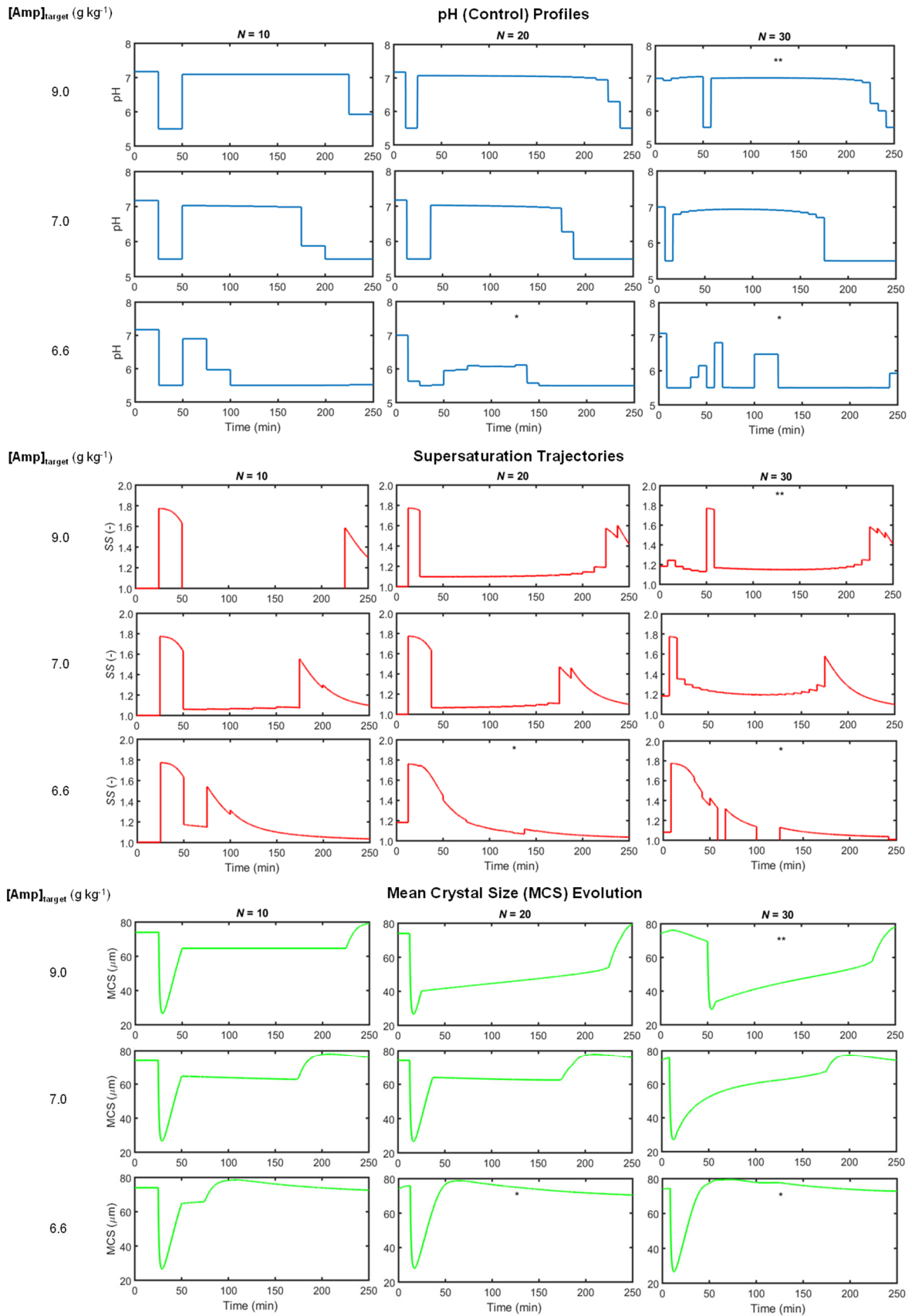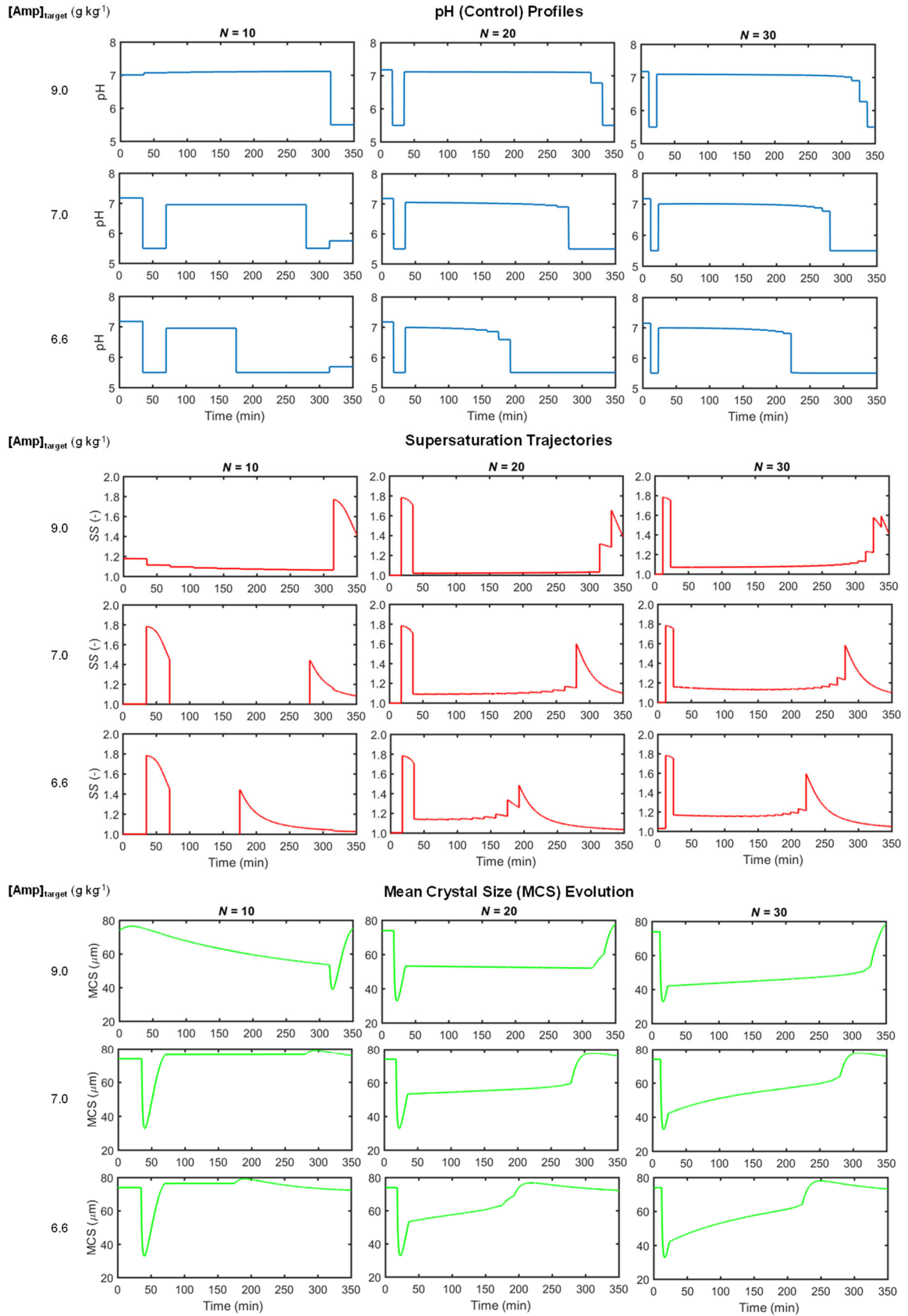
Figure 5: Optimization results for Case 1. Objective function weights, W_{STD} = 1.0, W_{MCS} = 1.5, no. state variable collocation points K_x = 3, initialization pH(t) profile = 7 (*: initialized at constant $pH(t)$ = 6. **: K_x = 6).

Figure 6: Optimization results for Case 2. Objective function weights, $W_{STD} = 1.0$, $W_{MCS} = 1.5$, no. state variable collocation points $K_x = 3$, initialization pH(t) profile = 7.

When the weight on *MCS* in the objective function (W_{MCS}) is increased from 0.5 to 1.5 (see Supporting Information), control and state profiles maintain the same general form but contain some slight differences. For higher *MCS* weights, the same pH drop towards the end of the batch run is observed, but the magnitude of the drop is not as great, i.e., the pH is not dropped to as low a value as when W_{MCS} = 0.5 (Fig. 5). This result is observed as when *MCS* is given greater importance in the objective function (i.e., higher W_{MCS}), a lower drop in pH promotes nucleation less, i.e., forms fewer nuclei and allows for a higher *MCS*. This effect is also observed in the generated *MCS* evolution profiles, where the final *MCS* is higher.

Increasing *N* increases the number of equispaced time segments in which the pH is piecewise constant. The lowest discretization (*N* = 10) is sufficient to capture the general behaviour as higher discretization levels, but not the more detailed fluctuations established as optimal by the dynamic optimization solver. The choice of *N* should also account for feasible control responses implementable in practical application, i.e., how fast pH can be varied by controllers in reality.

The step-size (Δt) in the implemented dynamic optimization varies between different cases (which have different final time durations, t_f, listed in Table 5 of the revised manuscript) and considered discretization level, *N* = {10, 20, 30}, but is not considered as a decision variable. Considering Δt as a decision variable increases problem complexity and may allow further artificial improvement of the objective function, but it is also critical to remark that below a certain value (equal to the fastest intrinsic timescale of the process, as per the concurrent mass, momentum and reactive transport phenomena), unrealistically short timesteps are inoperable, due to the inherent thermal/mass transfer inertia of bioreactors and fermentors (cf. relevant remarks in prior studies, Rodman & Gerogiorgis, 2016-19).

Addition of pH dynamic equations to the model can allow for a comparison with the immediate pH response assumption. Varying weights on the *MCS* component of the objective function have also been considered. Generally, the same trends and optimal system manipulations and behaviors are observed. An objective function considering both *MCS* and *STD* are important, as both are essential quality attributes in pharmaceutical crystalline products. The weighted objective used in this work for minimization is formulated for the purposes of a multiobjective optimization, i.e., maximization of *MCS* and minimization of *STD*, using a single function. Other options may also be implemented for bicriteria optimization problems, e.g, ε-constraint approaches, wherein one objective can be considered as a constraint while the other is solved to optimality.[33] Such approaches avoid potential arbitrary in selecting objective function component weights a priori. Nevertheless, the method implemented in this work is valid for formulation of a bicriteria objective function which captures two essential attributes of pharmaceutical solid products.

Optimization results for Case 2 are shown in Fig. 6. For both W_{MCS} values considered, the pH drop towards the end of the batch duration is observed later than in Case 1. The likely cause of this is the higher seed loading; the yield is enhanced by increased seed loading and thus fewer nuclei are needed to meet the specified yield constraint. The attained crystallization yield is calculated from the final solute concentration in the product solution vs. that fed in the crystal-free feed mother liquor. It is observed that the attained crystallization yield is high for cases with higher seed loading. Other trends observed are as per Case 1.

Optimal trajectories of pH, *SS* and *MCS* for Case 3 are shown in Fig. 8. In all cases, a pH drop is only implemented towards the end of the batch duration. This is likely a consequence of implementing a significant seed loading (15 wt%) compared to Cases 1 and 2. As the seed loading is very high, the crystallization yield is already high and thus crystal growth is more important that generating new nuclei in this case (as per the objective function). The *MCS* evolution generally decreases over time, with some cases having the final *MCS* value lower than the average seed crystal size; this result highlights the need for selection of appropriate seed loading and average seed crystal sizes as well as pH profile selection for optimal batch crystallization process design. Investigating seed size selection and dynamic seeding optimization may yield more materially efficient operating policies for ampicillin crystallization.[26]

Unless otherwise highlighted in Figs. 5–10, optimization runs were performed using K_x = 3 collocation points with an initially constant (i.e., non-dynamic) pH = 7. Certain problem instances required K_x = 6 collocation points in order to converge due to the higher accuracy/greater degree of approximation of the ODEs to algebraic equations; of course, this increase in accuracy is at the cost of more expensive computations and longer run times. The effect of initialization strategies on the optimal solutions may also be investigated to a greater degree and more systematically in future work.
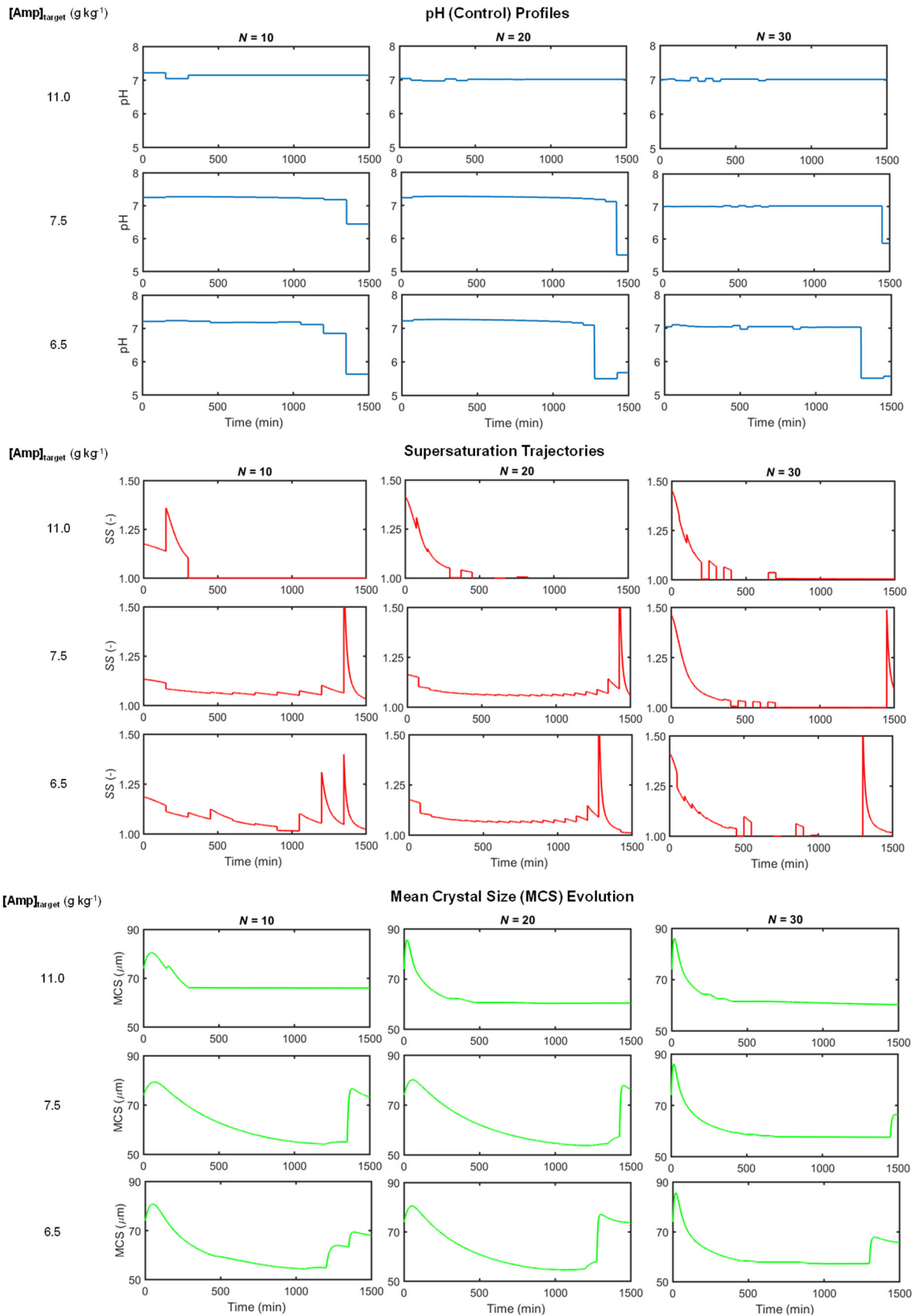
Figure 7: Optimization results for Case 3. Objective function weights, $W_{STD} = 1.0$, $W_{MCS} = 1.5$, no. state variable collocation points $K_x = 3$, initialization pH(t) profile = 7.

14

The currently implemented model assumes that pH change in the crystalliser mother liquor mixture is instantaneous, i.e., there is no explicit pH variation ODE incorporated into the dynamic model which accounts for a lag in change due to mixing of acid/base into solution. Incorporation of such a model will lead to different solutions than those presented here for different considered scenarios. The presented optima also assume that rapid monitoring is available; implementation of Process Analytical Technology (PAT) for rigorous control and analysis has been demonstrated in numerous publications in the literature and should be used wherever possible.[34–36]

The mother liquor solution fed to the crystallizer only considers ampicillin being crystallised without any impurities which will inherently be present in practical applications, e.g., a crystallization operation following synthesis of the antibiotic. Considering the effects of impurities on crystallization performance requires data on component partitioning between mother liquor (liquid) and crystalline product (solid) phases, or explicit crystallization kinetics for the impurity components themselves as well as those for the desired antibiotic molecule.[13] One method of circumventing impurity accumulation and solvent occlusion in the crystalline produce is reactive crystallization, a form of process intensification which has been implemented in the literature for β-lactam antibiotic molecules and other pharmaceutical compounds.[37–39] Reactive crystallization requires that the ratios of reaction to mass transfer and crystallization be ensured such that the mixture supersaturation is not so high as to result in excessive nucleation and thus wide size distributions.[27]
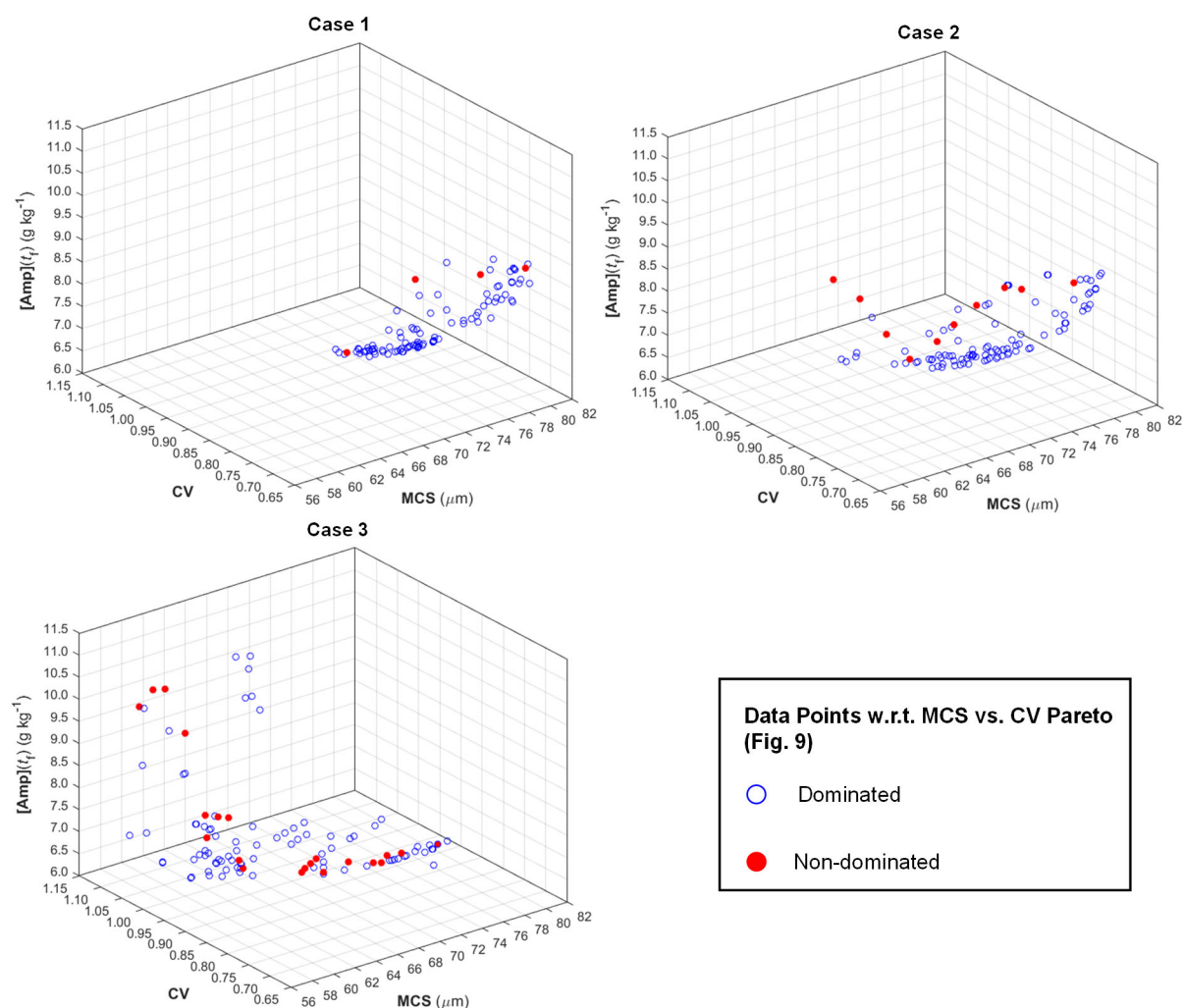

Figure 8: 3D Pareto front of the multiobjective optimisation problem for all cases.

3.2.   Pareto Fronts

A Pareto front represents a set of non-dominated solutions in a multiobjective optimization problem, where non-dominated solutions are those where no single objective can be improved without sacrificing at least one other objective. Comparison of Pareto fronts for different manufacturing scenarios are useful for visualisation and elucidation of the nature of trade-offs in multiobjective optimisation problems.[40–42] Pareto fronts of the attained ampicillin concentration with respect to *MCS* and *CV* are developed to quantify, visualise and highlight trade-offs between different product quality attributes of the batch ampicillin crystallization process. In Fig. 8, the 3D Pareto fronts for different seeded crystallization cases is presented, with 2D representations of the Pareto front from different perspectives ($[Amp](t_f)$ vs. *MCS* and $[Amp](t_f)$ vs. *CV*) shown in Figs. 9 and 10. Figs. 8–10 show non-dominating solutions from the *MCS* vs. *CV* 2D Pareto front (Fig. 12) highlighted in red, with dominated solutions in blue.
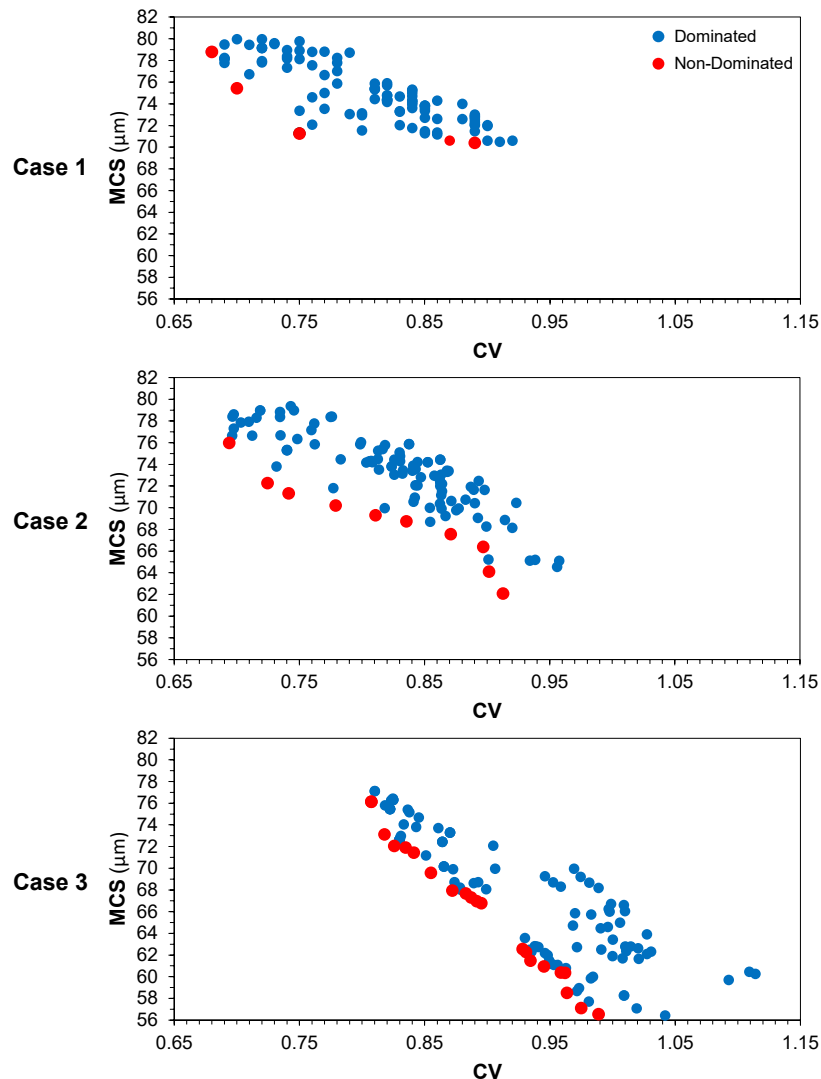

Figure 9: 2D Pareto front of the multiobjective optimisation problem for all cases: *MCS* vs. *CV*.

In Fig. 8, it is observed for lower seeding concentrations (i.e., Cases 1 and 2) that attained *MCS* and *CV* values are higher and lower, respectively, than for higher seed loading cases (Case 3). For Case 3, in some (dominated) cases the final *MCS* attained is lower than the seed crystal size; a possible method for mitigating this in the optimization problem formulation is to specify that the *MCS* should be larger than the seed size via an additional constraint to the problem. It is also observed for Case 3 that there is not as evident a tradeoff between yield and *MCS* or *CV*. As mentioned previously, investigating the effect of intermediate seed loadings and the effect of dynamic seeding policies will help to further our understanding of the process. However, the main purpose of this work was to establish novel optimal pH control profiles for product quality attribute (size and distribution width) optimisation subject to

various yield constraints for comparison with experimental demonstrations of different seeded crystallisation cases for ampicillin.

Fig. 9 shows 2D projections of *MCS* vs. *CV* from the 3D projections in Fig. 8 for different cases considered. It is desirable to have a high *MCS* but low *CV* (i.e., narrow size distribution); it is seen from Fig. 9 that only a small number of the non-dominated solutions from Fig. 8 are non-dominated with respect to *MCS* and *CV* for all cases. For lower seed loading cases (1 and 2), the front of high *MCS* / low *CV* generally allows for better values in both objectives compared to Case 3, which has a higher seed loading. Trade-offs in these objectives and required values depends on the implemented downstream unit processes for ampicillin. Ampicillin is most commonly administered orally and so considerations of the effect of downstream processes on drug product dissolution kinetics and bioavailability are an important consideration.

In Fig. 10, the observed Pareto fronts show the tradeoff between the considered performance metrics. Evidently, increasing the crystallization yield (i.e., decreasing the final ampicillin concentration in solution) is at the expense of a wider size distribution (i.e., a higher *CV*) and vice versa. This trend is a result of the fact that high yields require high nucleation vs. growth rates, which results in lower *MCS* and wider distributions. The gradient of the front is important in choosing an operating point; where the slope is shallow represents areas where reductions in *CV* (desirable) can be made without significant detriment to the crystallization yield. The pH profiles for labeled non-dominated solutions are also presented. The required *MCS* is dependent on downstream unit operations for formulation; additional information on specific requirements will narrow the number of feasible optimal operating points.
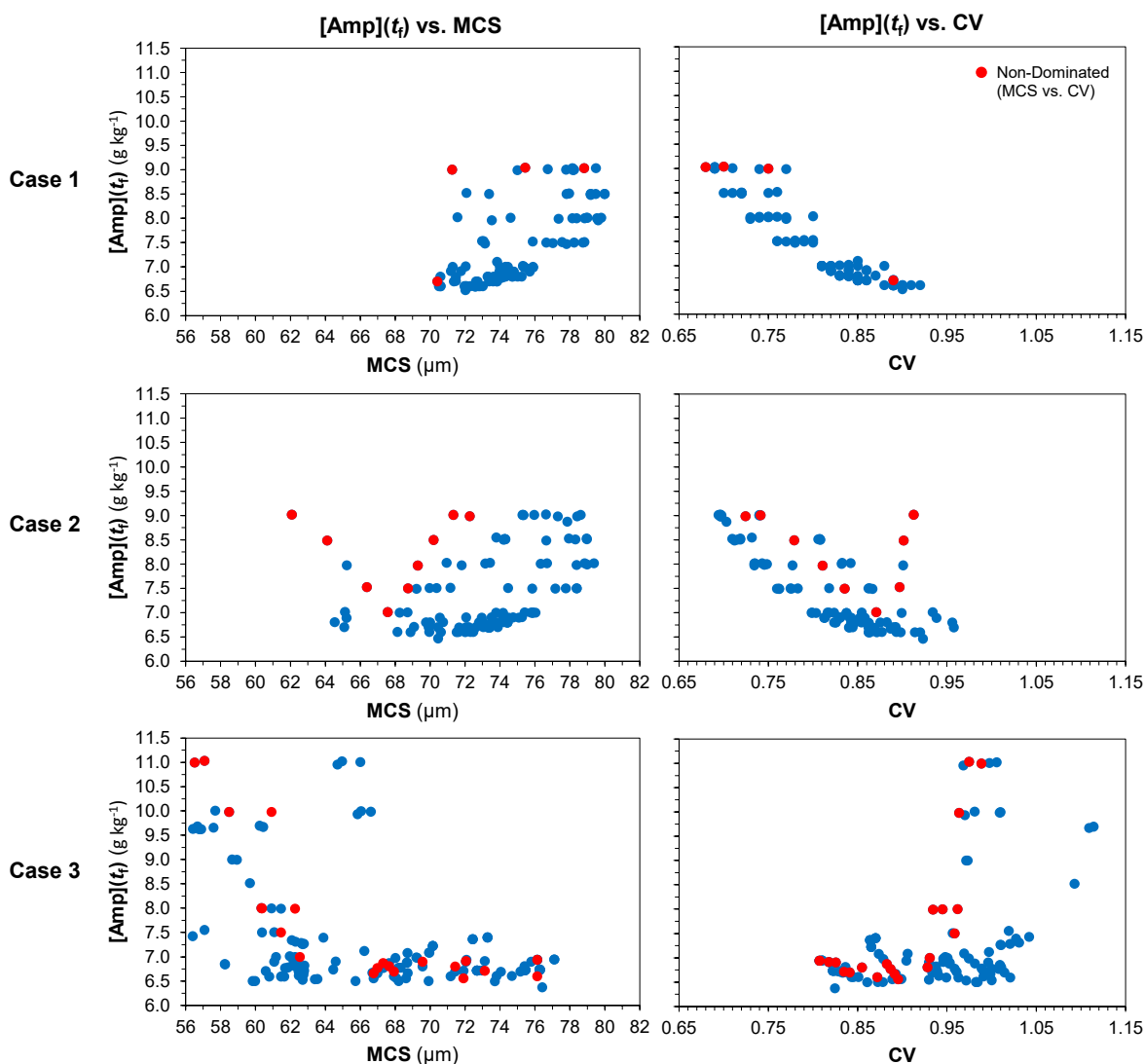

Figure 10: 2D Pareto front projections for different cases.

4.   Conclusions

This work implemented dynamic optimization results for the batch crystallization of ampicillin via pH control. A recently published crystallization model describing ampicillin solubility, crystallization kinetics and population and mass balances was implemented. Dynamic simulations were conducted for design space investigation prior to dynamic optimization of different batch crystallization processes. A dynamic optimization problem for an objective function weighted in both the mean crystal size and size distribution width subject to different yield constraints was then formulated and solved for different seeded crystallization cases implemented in the literature. Optimization results show an initial pH drop (i.e. higher supersaturation) is necessary to induce primary and secondary nucleation, with a subsequent increase in pH (lower supersaturation) to promote growth of the formed nuclei. Then an intermediate phase is observed where is pH gradually decreased, the magnitude of which depends on the target yield of the crystallization process. This form of control profile allows for controlled supersaturation to enhance crystal growth. At the end of the intermediate phase a final pH drop is observed, forcing more product to crystallise in order to achieve the yield constraint whilst maximizing the quality attributes forming the optimization objective function. Future work can also consider the amount of seeding as a dynamic control variable to further elucidate optimal dynamic control profiles to meet different production specifications of ampicillin production.

Associated Content
Supporting Information
Optimal pH manipulation trajectories, supersaturation profiles and Mean Crystal Size (MCS) evolutions for different seed loading (Cases 1–3), final ampicillin concentration constraint ($[Amp]_{target}$), number of discretization elements (N) and objective function component weights (W). This information is available free of charge via the Internet at http://pubs.acs.org/.

Author Information
Corresponding Author
Email: D.Gerogiorgis@ed.ac.uk
Phone: *+ 44 131 6517072*
ORCID ID: Dimitrios I. Gerogiorgis: 0000-0002-2210-6784

Nomenclature
Acronyms
API	Active Pharmaceutical Ingredient
COBC	Continuous Oscillatory Baffled Crystallizer
CSD	Crystal Size Distribution
CV	Coefficient of Variation
FDA	Food and Drug Administration
MCS	Mean Crystal Size
MSMPR	Mixed Suspension, Mixed Product Removal
NLP	Nonlinear Programming
ODE	Ordinary Differential Equation
PDE	Partial Differential Equation

PFC	Plug Flow Crystallizer
PWC, PWL	Piecewise Constant, Piecewise Linear
WHO	World Health Organization

Variables

Latin Letters

$[Amp]_0$	Concentration of ampicillin in the mother liquor at t_0 (g kg^{-1})
b	Secondary nucleation mass exponent ($-$)
B_0	Primary nucleation constant ($-$)
B_1, B_2	Primary, secondary nucleation rate (# crystals (g kg^{-1})$^{-1}$ min^{-1})
f	Optimization objective function
G	Crystal growth rate (m min^{-1})
g	Growth rate exponent ($-$)
J	Total nucleation rate (# crystals (g kg^{-1})$^{-1}$ min^{-1})
K_{A1}, K_{A2}	Acid, Amine protonation equilibrium constant
k_B	Boltzmann constant (m^2 kg s^{-2} K^{-1})
k_{B1}, k_{B2}	Primary, secondary nucleation rate constant (# crystals (g kg^{-1})$^{-1}$ min^{-1})
K_D	Equilibrium constant of neutral ampicillin molecules
k_G	Growth rate constant (m min^{-1})
K_U, K_x	Number of control, state variable collocation points ($-$)
k_V	Crystal volume shape factor ($-$)
L	Characteristic crystal length (m)
$\bar{L}_{seed}$	Average seed crystal characteristic length (m)
M	Crystalliser suspension density (g kg^{-1})
m_i	i^{th} moment of the population balance
m_{sol}	Mass of solution (kg)
n	Population density (# crystals m^{-1} g kg^{-1})
N	Number of discretized time intervals ($-$)
N_A	Avogadro number (mol^{-1})
n_0	Initial population density (# crystals m^{-1} g kg^{-1})
p_i	Scaling parameter for moment i ($-$)
$pH(t)$	pH value at time t ($-$)
pI	Isoelectric point of ampicillin ($-$)
R^2	Coefficient of determination
S	Solubility of ampicillin in water (g kg^{-1})
s	Secondary nucleation supersaturation exponent ($-$)
SS	Ampicillin supersaturation in the mother liquor ($-$)
STD	Size distribution standard deviation
t	Time (min)
t_f	Batch duration (min)
t_0	Initial time point = 0 (min)
T	Temperature (K)
$u(t)$	Control variable
W_j	Weight on variable j in the objective function
$x(t)$	State variables

Greek Letters

ε	Van der Waals attractive interaction parameter (m^2 kg s^{-2})
λ	Pitzer binary interaction parameter (kg mol^{-1})
ρ_c	Ampicillin crystal (kg m^{-3})
σ	Van der Waals diameter (m)

References

(1) Zaffiri, L.; Gardner, J.; Toledo-Pereyra, L.H. History of antibiotics. From salvarsan to cephalosporins. *J. Investig. Surg.* **2012**, *25*(2), 67–77.

(2) Kong, K.F.; Schneper, L.; Mathee, K. Beta-lactam antibiotics: from antibiosis to resistance and bacteriology. *APMIS* **2010**, *118*(1), 1–36.

(3) Pulcini, C.; Beovic, B.; Béraud, G.; Carlet, J.; Cars, O.; Howard, P.; Levy-Hara, G.; Li, G.; Nathwani, D.; Roblot, F.; Sharland, M. Ensuring universal access to old antibiotics: a critical but neglected priority. *Clin. Microbiol. Infect.* **2017**, *23*(9), 590–592.

(4) World Health Organisation (WHO). *WHO Report on Surveillance of Antibiotic Consumption*; 2018.

(5) Hamed, R.B.; Gomez-Castellanos, J.R.; Henry, L.; Ducho, C.; McDonough, M.A.; Schofield, C. J. The enzymes of β-lactam biosynthesis. *Nat. Prod. Rep.* **2013**, *30*(1), 21–107.

(6) Chianese, A.; Kramer, H.J.M. *Industrial Crystallization Process Monitoring and Control*; Chianese, A., Kramer, H.J.M., Eds.; Wiley-VCH Verlag GmbH & Co. KGaA: Weinheim, Germany, 2012.

(7) Chen, J.; Sarma, B.; Evans, J.M.B.; Myerson, A.S. Pharmaceutical crystallization. *Cryst. Growth Des.* **2011**, *11*(4), 887–895.

(8) Nagy, Z.K.; Fujiwara, M.; Braatz, R.D. Modelling and control of combined cooling and antisolvent crystallization processes. *J. Process Control* **2008**, *18*(9), 856–864.

(9) Lindenberg, C.; Krättli, M.; Cornel, J.; Mazzotti, M.; Brozio, J. Design and optimization of a combined cooling/antisolvent crystallization process. *Cryst. Growth Des.* **2009**, *9*(2), 1124–1136.

(10) Ridder, B.J.; Majumder, A.; Nagy, Z.K. Population balance model-based multiobjective optimization of a multisegment multiaddition (MSMA) continuous plug-flow antisolvent crystallizer. *Ind. Eng. Chem. Res.* **2014**, *53*(11), 4387–4397.

(11) Acevedo, D.; Tandy, Y.; Nagy, Z.K. Multiobjective optimization of an unseeded batch cooling crystallizer for shape and size manipulation. *Ind. Eng. Chem. Res.* **2015**, *54*(7), 2156–2166.

(12) Rasche, M.L.; Jiang, M.; Braatz, R.D. Mathematical modeling and optimal design of multi-stage slug-flow crystallization. *Comput. Chem. Eng.* **2016**, *95*, 240–248.

(13) Li, J.; Lai, T.C.; Trout, B.L.; Myerson, A.S. Continuous crystallization of cyclosporine: the effect of operating conditions on yield and purity. *Cryst. Growth Des.* **2017**, *17*(3), 1000–1007.

(14) Diab, S.; Gerogiorgis, D.I. Technoeconomic optimization of continuous crystallization for three active pharmaceutical ingredients (APIs): cyclosporine, paracetamol and aliskiren. *Ind. Eng. Chem. Res.* **2018**, *57*(29), 9489–9499.

(15) Jolliffe, H.G.; Gerogiorgis, D.I. Process modelling, design and technoeconomic evaluation for continuous paracetamol crystallisation. *Comput. Chem. Eng.* **2018**, *118*, 224–235.

(16) Pal, K.; Yang, Y.; Nagy, Z.K. Model-based optimization of cooling crystallization of active pharmaceutical ingredients undergoing thermal degradation. *Cryst. Growth Des.* **2019**, *19*(6), 3417–3429.

(17) Gao, Z.; Rohani, S.; Gong, J.; Wang, J. Recent developments in the crystallization process: toward the pharmaceutical industry. *Engineering* **2017**, *3*(3), 343–353.

(18) Encarnación-Gómez, L.G.; Bommarius, A.S.; Rousseau, R.W. Crystallization kinetics of ampicillin using online monitoring tools and robust parameter estimation. *Ind. Eng. Chem. Res.* **2016**, *55*(7), 2153–2162.

(19) Hogiri, T.; Tamashima, H.; Nishizawa, A.; Okamoto, M. Optimization of a pH-shift control strategy for producing monoclonal antibodies in chinese hamster ovary cell cultures using a ph-dependent dynamic model. *J. Biosci. Bioeng.* **2018**, *125*(2), 245–250.

(20) De Pessôa Filho, P.A.; Maurer, G. An extension of the pitzer equation for the excess gibbs energy of aqueous electrolyte systems to aqueous polyelectrolyte solutions. *Fluid Phase Equilib.* **2008**, *269*(1–2), 25–35.

(21) Rudolph, E.S.J.; Zomerdijk, M.; Ottens, M.; van der Wielen, L.A.M. Solubilities and partition coefficients of semi-synthetic antibiotics in water + 1-butanol systems. *Ind. Eng. Chem. Res.* **2001**, *40*(1), 398–406.

(22) Santana, M.; Ribeiro, M.P.A.; Leite, G.A.; Giordano, R.L.C.; Giordano, R.C.; Mattedi, S. Solid-liquid equilibrium of substrates and products of the enzymatic synthesis of ampicillin. *AIChE J.* **2010**, *56*(6), 1578–1583.

(23) Florey, K.; Brewer, G.A.; Cohen, E.M.; Guttman, D.E.; Olin, S.M.; Papariello, G.J.; Florey, K.; Fusari, S.A. *Analytical Profiles of Drug Substances*. **1973**, *2*, 4–61.

(24) Dürr, R.; Kienle, A. An efficient method for calculating the moments of multidimensional growth processes in population balance systems. *Can. J. Chem. Eng.* **2014**, *92*(12), 2088–2097.

(25) Jha, S. K.; Karthika, S.; Radhakrishnan, T.K. Modelling and control of crystallization process. *Resour. Technol.* **2017**, *3*(1), 94–100.

(26) Chung, S.H.; Ma, D.L.; Braatz, R.D. Optimal seeding in batch crystallization. *Can. J. Chem. Eng.* **1999**, *77*(3), 590–596.

(27) Su, Q.L.; Braatz, R.D.; Chiu, M.-S. Concentration Control for semi-batch pH-shift reactive crystallization of L-glutamic acid. *IFAC Proc. Vol.* **2012**, *45*(15), 228–233.

(28) Ottens, M.; Lebreton, B.; Zomerdijk, M.; Rijkers, M.P.W.M.; Bruinsma, O.S.L.; van der Wielen, L.A. Impurity effects on the crystallization kinetics of ampicillin. *Ind. Eng. Chem. Res.* **2004**, *43*(24), 7932–7938.

(29) Giordano, R.C.; Ribeiro, M.P.A.; Giordano, R.L.C. Kinetics of β-lactam antibiotics synthesis by penicillin G acylase (PGA) from the Viewpoint of the industrial enzymatic reactor optimization. *Biotechnol. Adv.* **2006**, *24*(1), 27–41.

(30) McDonald, M.A.; Bommarius, A.S.; Rousseau, R.W. Enzymatic reactive crystallization for improving ampicillin synthesis. *Chem. Eng. Sci.* **2017**, *165*, 81–88.

(31) Bezerra, I.M.; Moreira, L.C.; Chiavone-Filho, O.; Mattedi, S. Effect of different variables in the solubility of ampicillin and corresponding solid phase. *Fluid Phase Equilib.* **2018**, *459*, 18–29.

(32) Čižniar, M.; Fikar, M.; Latifi, M.A. MATLAB Dynamic Optimisation Code DynOpt. User's Guide, Technical Report. *KIRP FCHPT STU Bratislava* **2005**.

(33) Marler, R.T.; Arora, J.S. Survey of multi-objective optimization methods for engineering. *Struct. Multidiscip. Optim.* **2004**, *26*(6), 369–395.

(34) Nagy, Z.K.; Fevotte, G.; Kramer, H.; Simon, L.L. Recent advances in the monitoring, modelling and control of crystallization systems. *Chem. Eng. Res. Des.* **2013**, *91*(10), 1903–1922.

(35) Yang, X.; Acevedo, D.; Mohammad, A.; Pavurala, N.; Wu, H.; Brayton, A.L.; Shaw, R.A.; Goldman, M.J.; He, F.; Li, S.; Fisher, R.J., O'Connor, T.F., Cruz, C.N. Risk considerations on developing a continuous crystallization system for carbamazepine. *Org. Process Res. Dev.* **2017**, *21*(7), 1021–1033.

(36) Yu, S.; Zhang, Y.; Wang, X.Z. Improved understanding of cefixime trihydrate reactive crystallization and process scale-up with the aid of PAT. *Org. Process Res. Dev.* **2019**, *23*(2), 177–188.

(37) McDonald, M.A.; Bommarius, A.S.; Rousseau, R.W.; Grover, M.A. Continuous reactive crystallization of β-lactam antibiotics catalyzed by penicillin G acylase. Part I: Model development. *Comput. Chem. Eng.* **2019**, *123*, 331–343.

(38) McDonald, M.A.; Bommarius, A.S.; Grover, M.A.; Rousseau, R.W. Continuous reactive crystallization of β-lactam antibiotics catalyzed by penicillin G acylase. Part II: Case study on ampicillin and product purity. *Comput. Chem. Eng.* **2019**, *126*, 332–341.

(39) Encarnación-Gómez, L.G.; Bommarius, A.S.; Rousseau, R.W. Reactive crystallization of β-lactam antibiotics: strategies to enhance productivity and purity of ampicillin. *React. Chem. Eng.* **2016**, *1*(3), 321–329.

(40) Reddy, M.J.; Kumar, D.N. Elitist-mutated multi-objective particle swarm optimization for engineering design. In *Encyclopedia of Information Science and Technology, Third Edition*; Mehdi Khosrow-Pour, D.B.A., Ed.; IGI Global: Hershey, PA, USA, 2015; 3534–3545.

(41) Rodman, A.D.; Gerogiorgis, D.I. Multi-objective process optimisation of beer fermentation via dynamic simulation. *Food Bioprod. Process.* **2016**, *100*, 255–274.

(42) Rodman, A. D.; Gerogiorgis, D. I. Dynamic optimization of beer fermentation: sensitivity analysis of attainable performance vs. product flavour constraints. *Comput. Chem. Eng.* **2017**, *106*, 582–595.